Supplementary Table 1. Related to Figure 1.

IG construct	Stoichiometry	Kd (μM)	ΔH Kcal/mol	ΔS cal/mol K
1483-1526	0.9	0.83	-5.2	10.2
1483-1523	0.7	1.1	-7.0	3.9
1483-1519	0.9	4.6	-3.2	13.5

Supplementary Table 2. Related to Figure 2.
Crystallographic data collection and refinement statistics.

PDB Entry	5DBR
Data collection	
Space group	$P3_221$
Cell dimensions	
a, b, c (Å)	58.09, 58.09, 102.64
α,β,γ (°)	90, 90, 120
Temperature (K)	100
Wavelength (Å)	1.542
Resolution (Å)	50.30 - 2.25 (2.31 - 2.25)
Reflections	
Total	167,361
Unique	19,561
Completeness (%)[a]	99.6 (100)
R_{merge} (%)[b]	9.1 (44.6)
I/σ	14.0 (1.9)
Redundancy	15.6 (10.6)
Refinement	
R_{work}/R_{free} (%)[c]	23.1/28.3
No. of residues	
Protein	145
IG Peptide	14
Solvent	11
Calcium	4
Average B-factor (Å^2)	
Protein	41.82
IG Peptide	39.21
Solvent	39.77
Calcium	38.59
RMSD bonds (Å)	0.018
RMSD angles (°)	1.913
Ramachandran[d]	
Most favored	135
Allowed	8
Disallowed	0

[a] Values in parentheses are for the highest-resolution shell.
[b] $R_{merge} = \Sigma(|I - \bar{I}|)/\Sigma I \times 100$.
[c] Rwork = $\Sigma|F_o - F_c|/\Sigma F_o \times 100$, where F_o is the observed structure factor amplitude and F_c is the calculated structure factor amplitude.
[d] Values are numbers of residues.

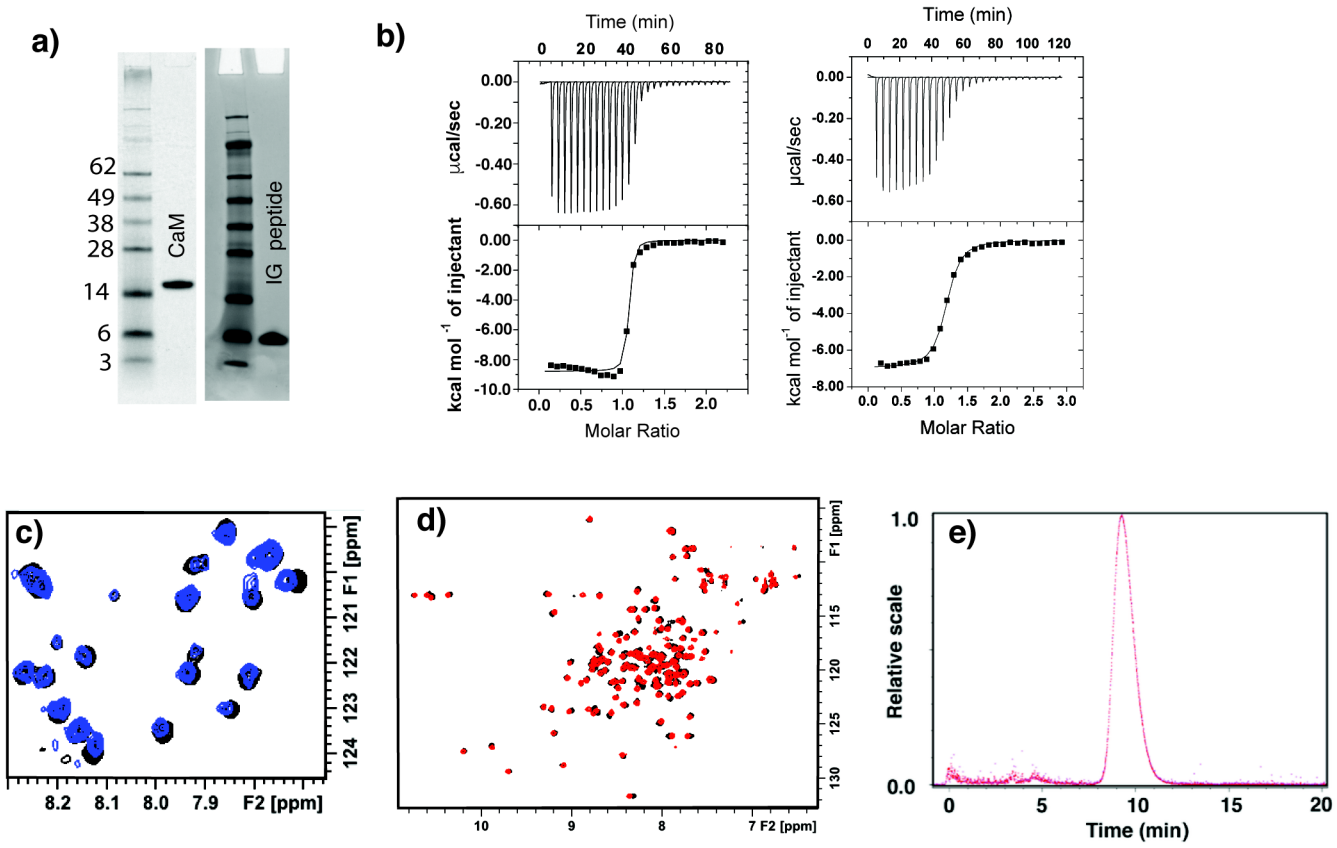

Fig. S1. Related to Fig. 1, Fig. 3, and Fig. 4. **Production and identification of an optimal IG construct**. a) 10% SDS denaturing gel of purified CaM and IG peptide. b) Sensorgrams and binding curves of CaM titrated into the $Na_V1.5$ D1471-D1532 peptide (left) and Q1483-A1529 (right). Conditions were 10 mM BIS-TRIS pH 6.5, 5 mM MES, 5 mM $CaCl_2$, and 20 mM TRIS, 50 mM NaCl, 1 mM $CaCl_2$ respectively. c) Overlay of ^{15}N-^{1}H HSQC NMR spectra of IG peptide in the absence (black) and presence (blue) of apo CaM. d) Overlay of ^{15}N-^{1}H HSQC spectra for Ca^{2+}-CaM with D1471-V1532 (black) and optimized Q1483-A1529 (red) -IG constructs. e) Size Exclusion Chromatography coupled to Multi-Angle Light Scattering (SEC-MALS) of the 1:1 Ca^{2+} CaM-IG complex.

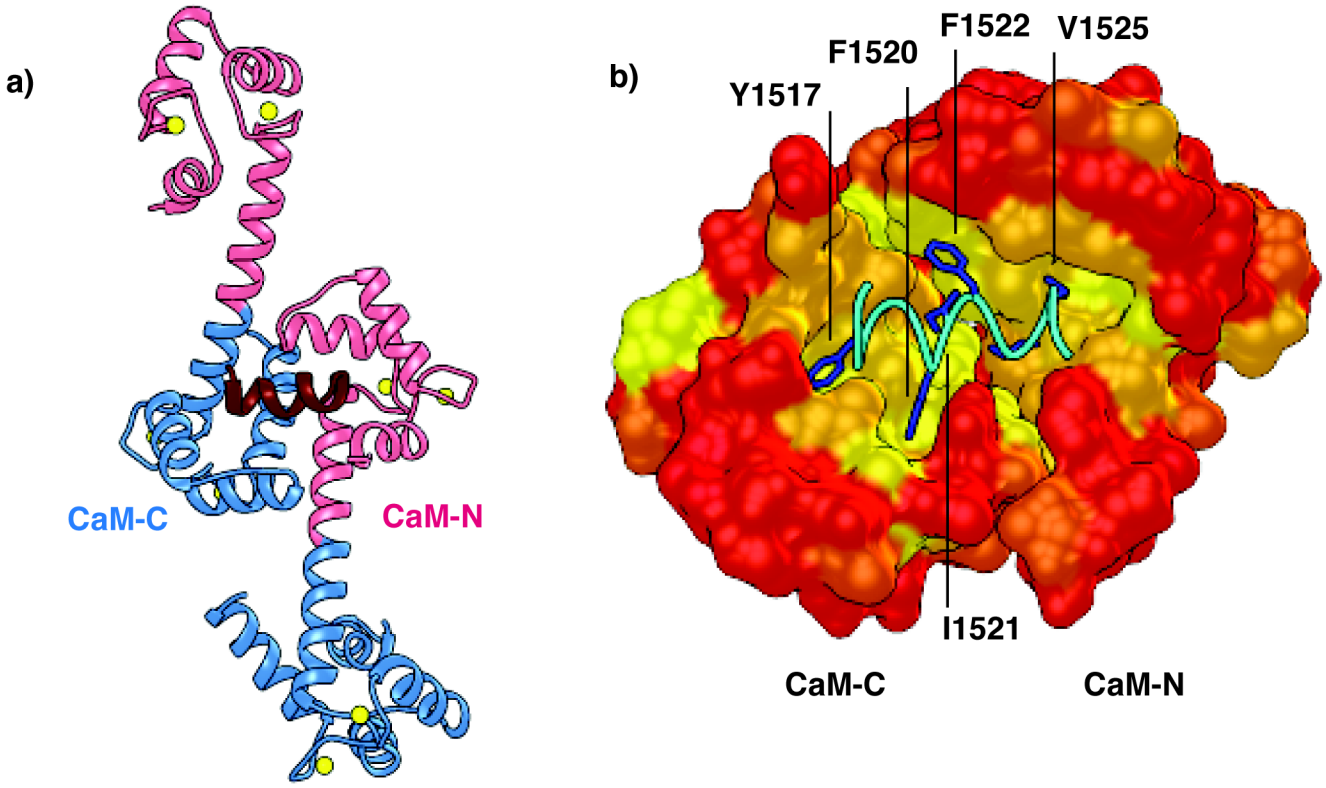

Fig. S2. Related to Fig. 2. **Crystal structure of CaM bound to $Na_V1.5$ IG peptide site B**. a) Density was observed for both CaM domains where adjacent molecules of CaM engaged IG L1514-T1526, consistent with a domain swap configuration. b) Surface rendering of CaM-N and -C domains color coded by hydrophobicity (red = least, yellow = most) bound to site B of IG peptide. IG peptide backbone shown

in cyan with interacting side chains in blue.

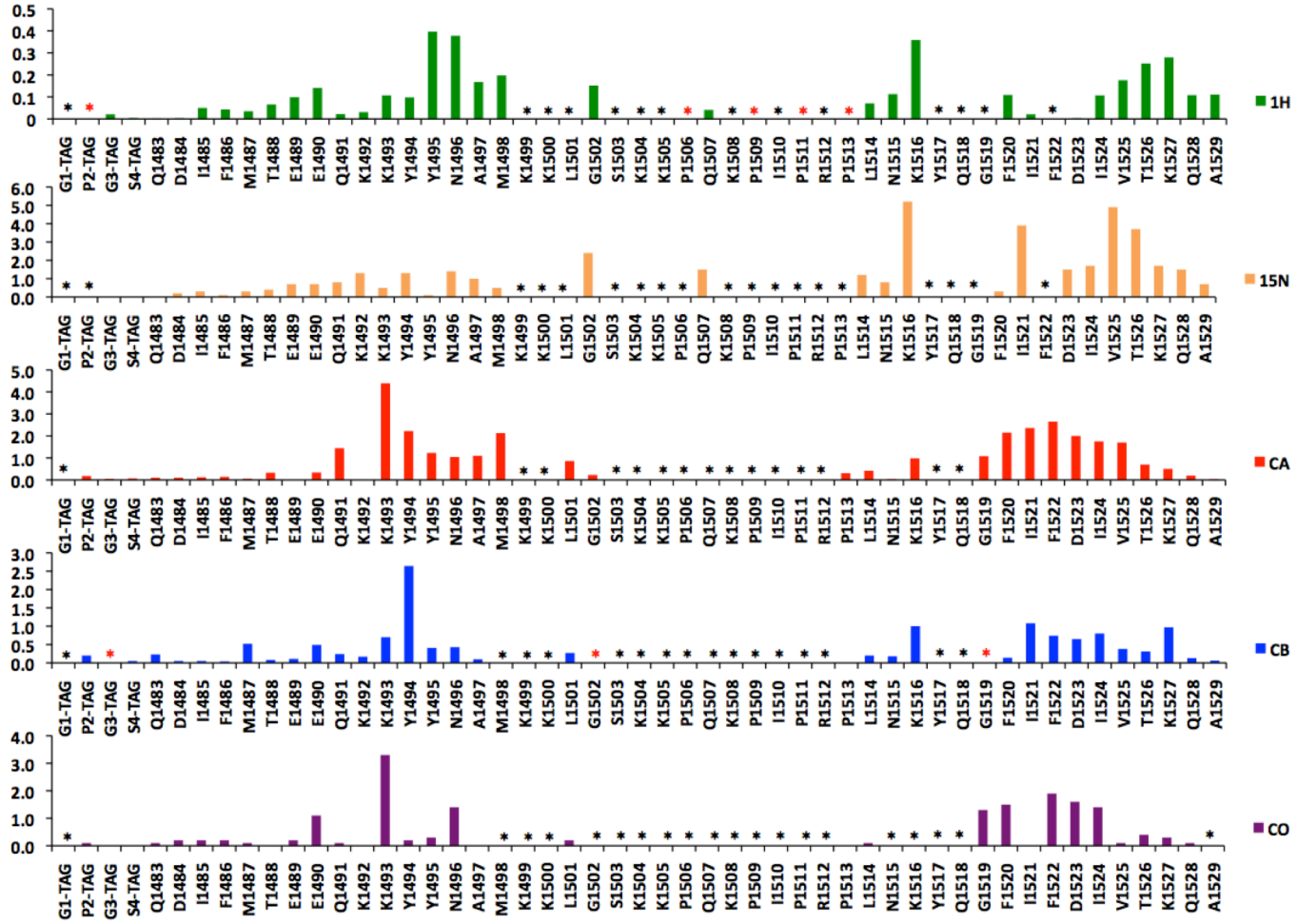

Fig. S3. Related to Fig. 3. **Expanded table of NMR chemical shift differences for the IG peptide in the absence and presence of Ca^{2+} CaM.** The * symbol denotes differences could not be calculated due to broadened or significantly overlapped resonances for either the free or complex IG samples. A red * symbol is used for the missing NH of Pro residues and CB of glycine residues.

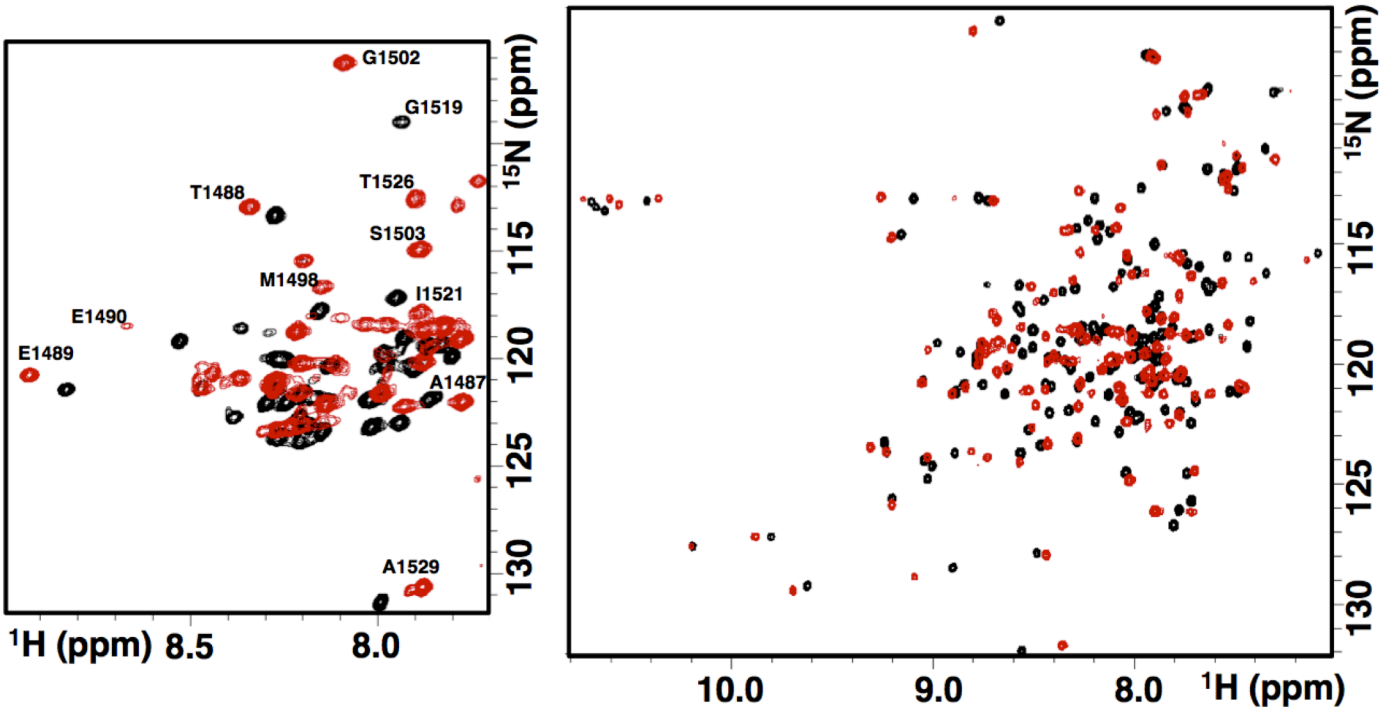

Fig. S4. Related to Fig. 3. **Expanded NMR spectra for IG peptide, CaM and complex.** Overlay of ^{15}N-^{1}H HSQC NMR spectra of the Q1483-A1529 IG peptide (left) in the absence (black) and presence (red) of Ca^{2+}-CaM. Overlay of ^{15}N-^{1}H HSQC NMR spectra of Ca^{2+}-CaM in the absence (black) and presence (red) of the Q1483-A1529 IG peptide. The spectra were acquired in a buffer containing 20 mM BISTRIS at pH 6.8, 100 mM KCl, and 2 mM CaCl2 at 310 K. Although complete resonance assignments were made for the IG peptide, only a subset is shown in the left panel for convenience.

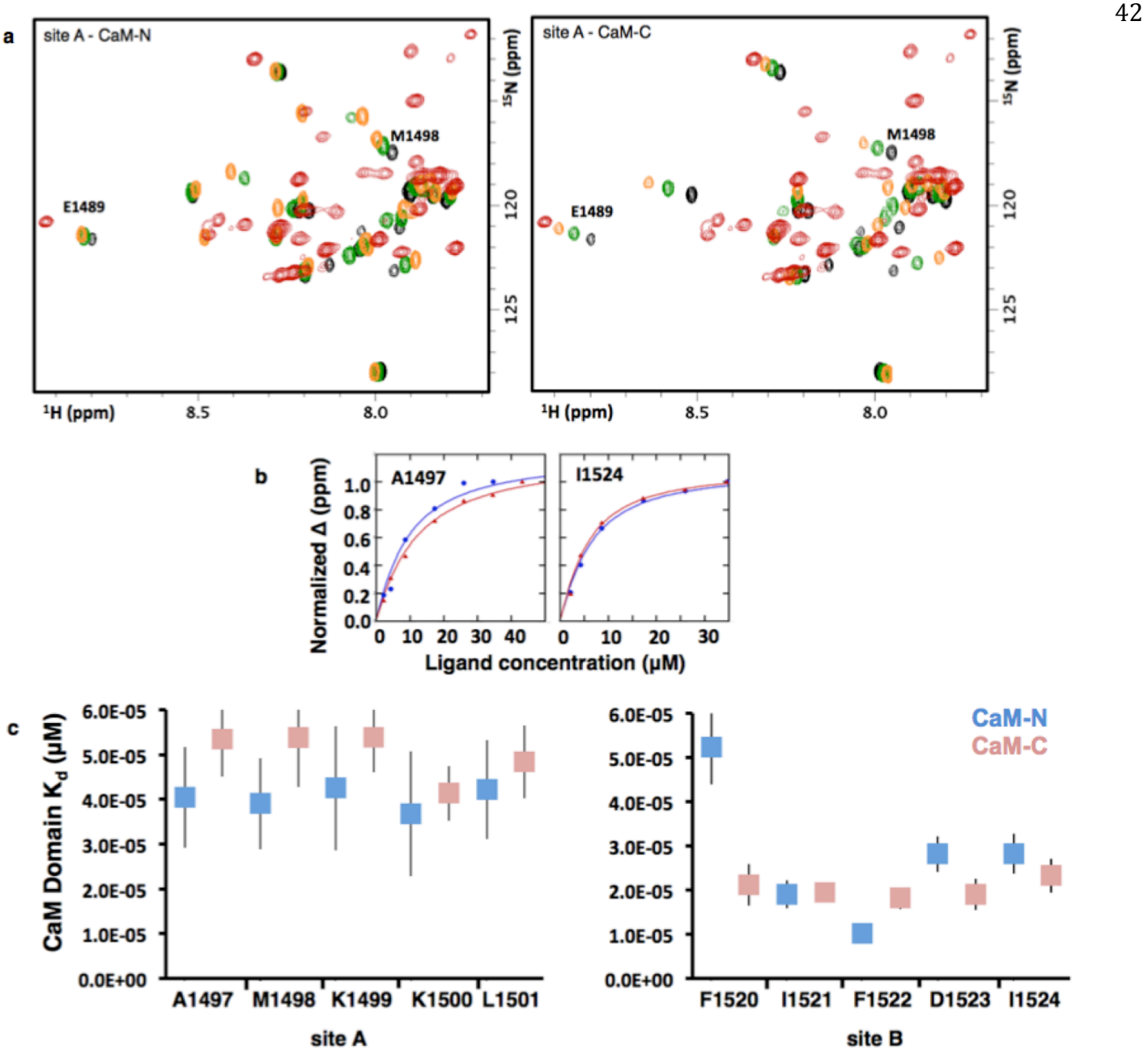

Fig. S5. Related to Fig. 1, and Fig. 3. **Interactions of Individual CaM domains and $Na_V1.5$ IG binding sites.** a) Overlay of ^{15}N-^{1}H HSQC spectra of $Na_V1.5$-IG site A peptide in the presence of Ca^{2+}-CaM –N (A1-M76) (left) and Ca^{2+}-CaM-C (K77-K148) (right). The spectra are colored in accord with CaM to peptide ratios of 0:1 (black), 2:1 (green), and 8:1 (orange). The spectra of full length CaM bound to the complete IG is overlaid in red. b) Binding curves from NMR chemical shift changes induced in IG peptides titrated with CaM-N (blue) and CaM-C (red). c) Summary of binding constants from the NMR titrations, residues of site A (left) and site B (right). Values for Q1491-Y1495 could not be determined due to significant spectral overlap. K_d values for CaM-N domain shown in blue and CaM-C domain shown in pink.

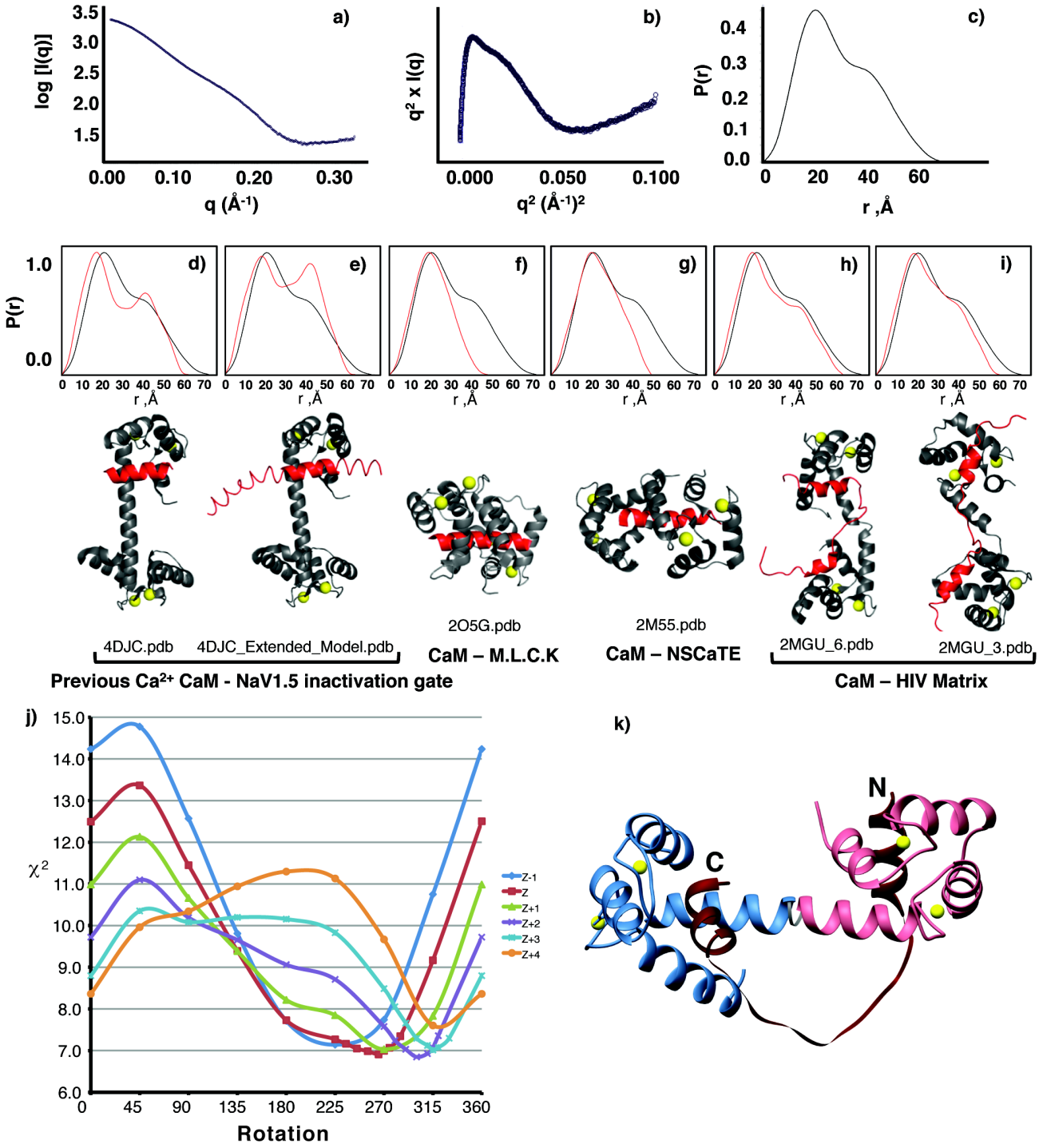

Fig. S6. Related to Fig. 4. **Expanded SAXS data for the CaM-IG complex and optimal orientation of the CaM -IG crystal structures.** a) intensity plot, b) Kratky-Debye plot, c) P(r), χ^2 = 0.84. d-i) Overlay of experimental P(r) (black) and back-calculated curves for different structures of CaM binding to peptides in different conformations (red). (J) Plot of χ^2 values for various orientations of the merged crystal structures for CaM-C -Site A and CaM-N -Site B interactions. (k) A minimum value is observed when the CaM domains are translated a distance of 2 Å closer together (purple line) and rotated ~300° about the central helix of CaM after alignment .

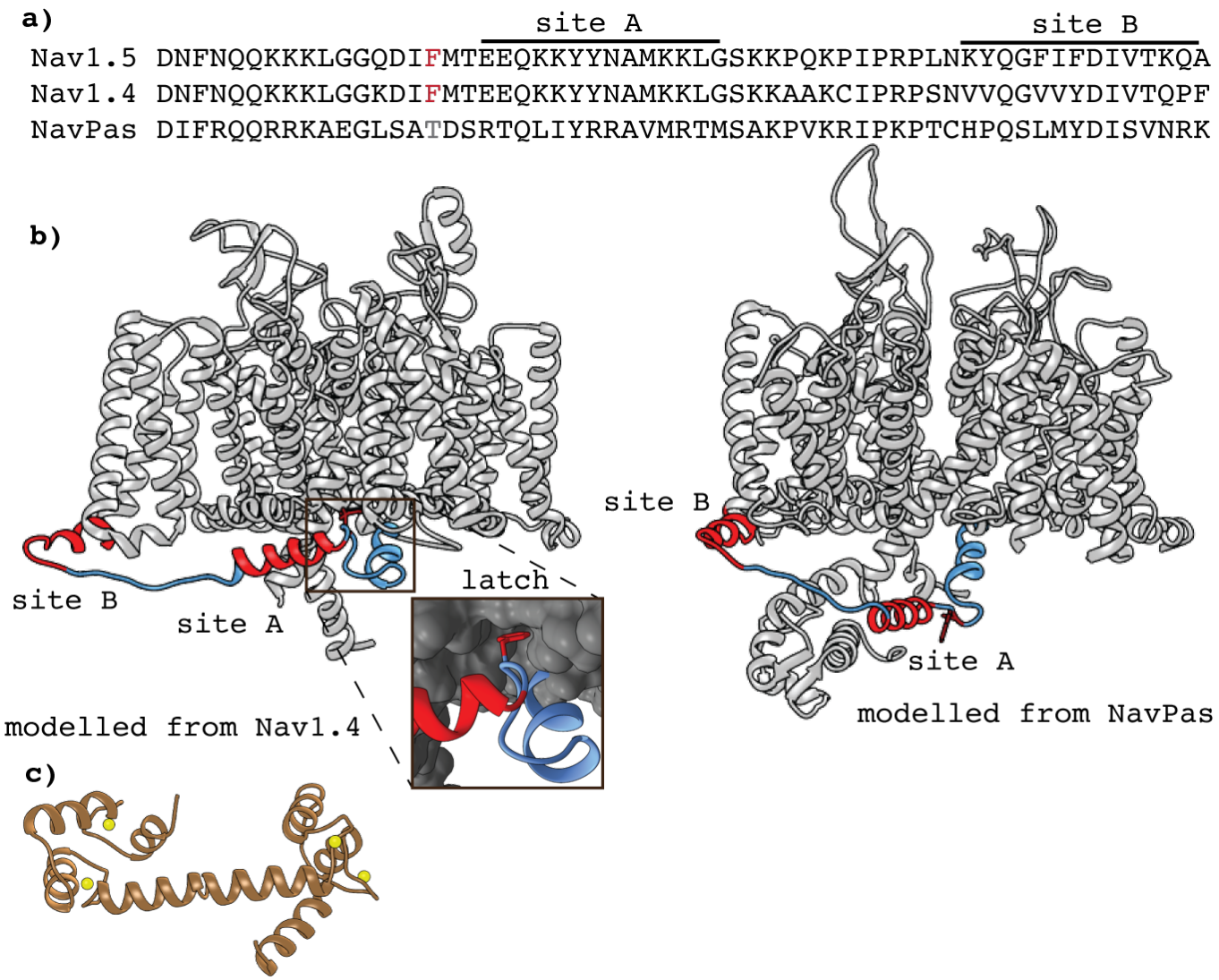

Fig. S7. Related to Fig. 6. **Homology of the $Na_V1.5$ alpha subunit.** a) Sequence alignment of IG sections from Na_V channels. b) Homology models of $Na_V1.5$ based on $Na_V1.4$ (left) and Na_VPas (right). The homology model of the alpha subunit from $Na_V1.5$ constructed from $Na_V1.4$ with the IG colored blue and CaM binding sites A and B highlighted in red. The latch F1486 is shown in dark red. The channel appears to be in the inactivated configuration and clearly CaM binding to the A and B sites would destabilize the latch interaction as well as re-orient site B portion of the IG. Both of these interactions would destabilize the structure of the suggested inactivated configuration. The Na_VPas channel contains minimal sequence and homology resemblance of the human $Na_V1.5$ IG sequence. Neither the latch or IG CaM bindings site sequences are conserved. The observed interaction between the EF hand and - Na_VPas IG occurs for an IG sequence that is not highly conserved in $Na_V1.5$. All homology models of $Na_V1.5$ indicate that both the IG A and B CaM binding sites are contained in the cytosol and not in the lipid bilayer. c) An extended structure of CaM is provided as a visual reference to illustrate that the -N and -C domains of CaM are able to span the distance between the two IG sites.

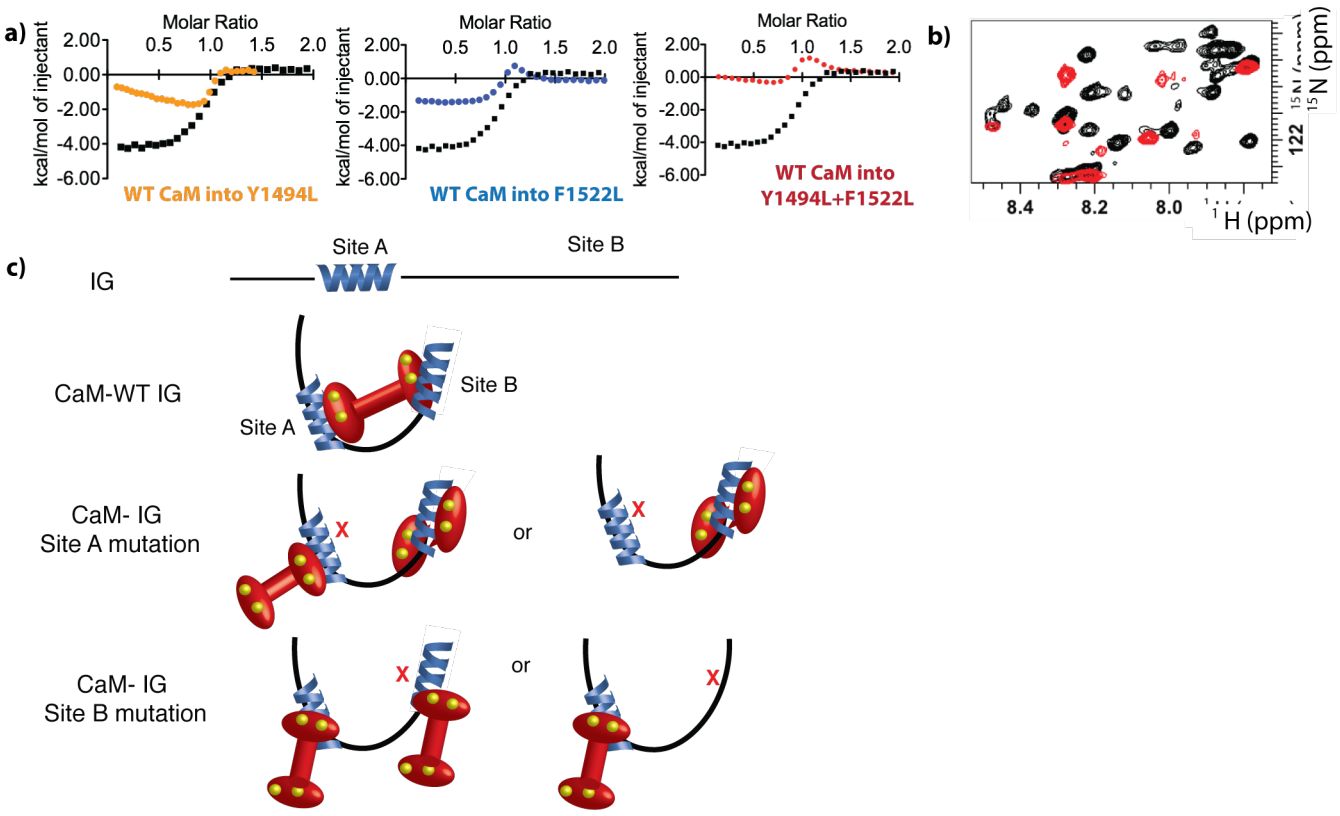

Fig. S8. Related to Fig. 7. In vitro characterization of the binding of CaM to the IG peptide variants. a) ITC sensorgrams for the three variants overlaid with CaM binding to WT IG (black). The sensorgram data could not be fit to a binding curve due to the complexity of the CaM interaction. We anticipate that the mutants reveal the existence of multiple equilibria because both CaM domains are able to interact with both IG binding sites, and CaM can also engage site B with a wrap around conformation. b) 2D NMR 15N-1H HSQC spectra of ^{15}N-enriched IG in complex with CaM (black) overlaid with the CaM complex with ^{15}N-enriched Y1494L+F1522L IG (red). For the double mutant numerous cross-peaks disappear upon the addition of CaM, consistent with an intermediate mode of exchange on the NMR timescale, whereas the WT IG peptide exhibits slow exchange. This difference is consistent with a reduction in the affinity of CaM for both sites A and B in the IG peptide. c) Schematic showing possible modes of CaM engaging an IG peptide containing a mutation at each binding site.

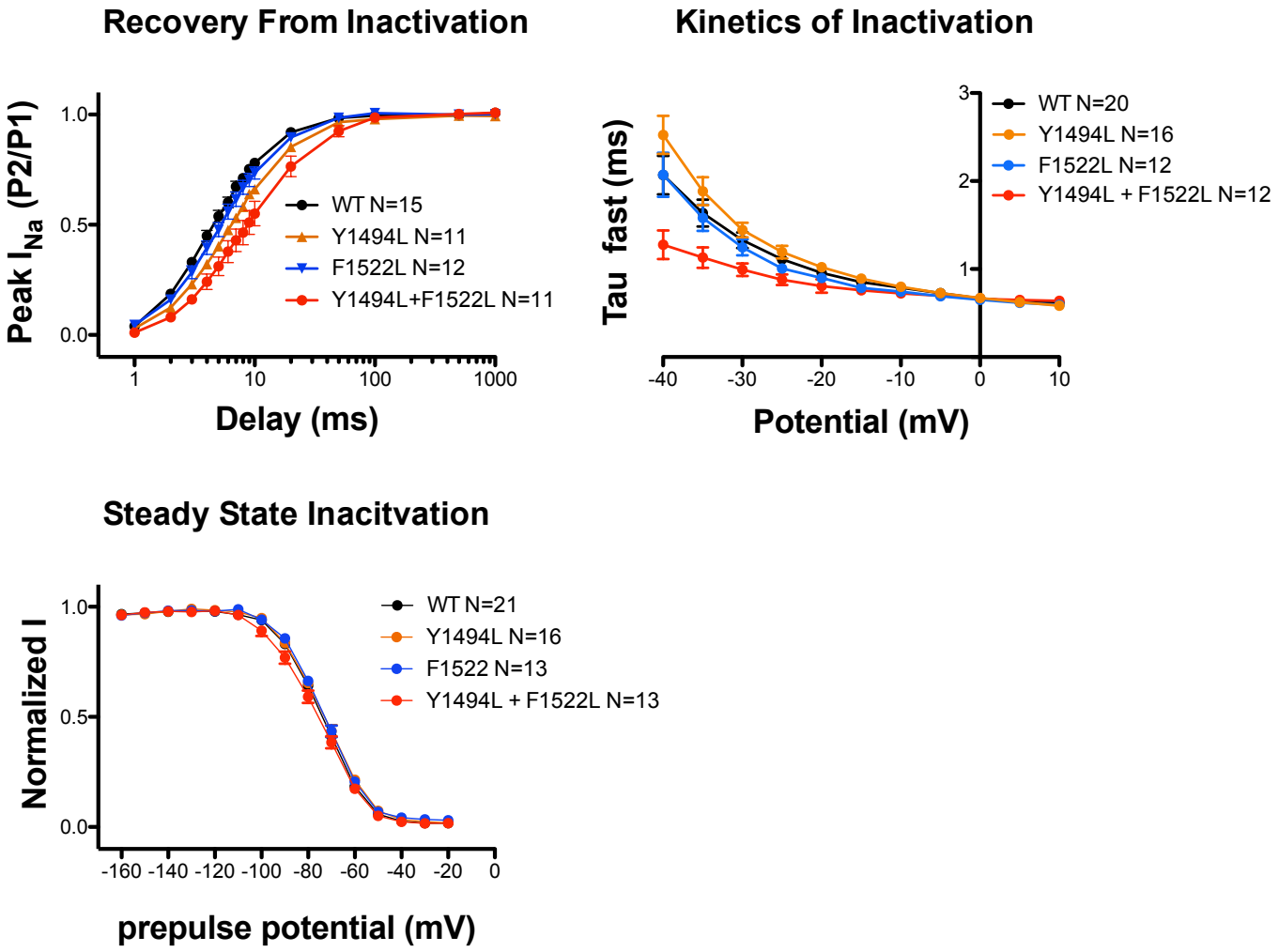

	Recovery (τ_{fast})	Recovery (τ_{slow})	Weight of fast component	Weight of slow component	Inactivation Kinetic (-30 mV) (τ_{fast})	$V_{1/2}$ steady-state Inactivation
WT	5.8 ± 0.5 ms n = 15	60.1 ± 4.9 ms n = 15	78 ± 3% n = 15	22 ± 3% n = 15	1.32 ± 0.08 ms n = 20	-73.7 ± 0.7 n = 21
Y1994L + F1522L	15.8 ± 4 ms* n = 12	156.1 ± 41 ms* n = 12	81 ± 3% n = 12	19 ± 3% n = 12	0.99 ± 0.07 ms* n = 12	-75.9 ± 1.4 n = 13
Y1494L	8.8 ± 0.4 ms* n = 11	112.7 ± 16.5 ms* n = 11	71 ± 2%* n = 11	29 ± 3%* n = 11	1.44 ± 0.08 ms n = 16	-73.0 ± 1.1 n = 16
F1522L	7.4 ± 0.7 ms n = 12	86.3 ± 10.1 ms* n = 12	82 ± 3% n = 12	18 ± 3% n = 12	1.24 ± 0.09 ms n = 12	-73.2 ± 1.1 n = 13

Fig. S9. Related to Fig. 7. **Whole cell patch clamp recordings of structure guided mutations.** Summary of recovery from inactivation, inactivation kinetic and voltage dependence of inactivation biophysical properties for $Na_V1.5$ WT, Y1994L + F1522L, Y1494L, F1522L, and Y1494N in presence of Ca^{2+}. *$P < 0.05$ (compared with WT)

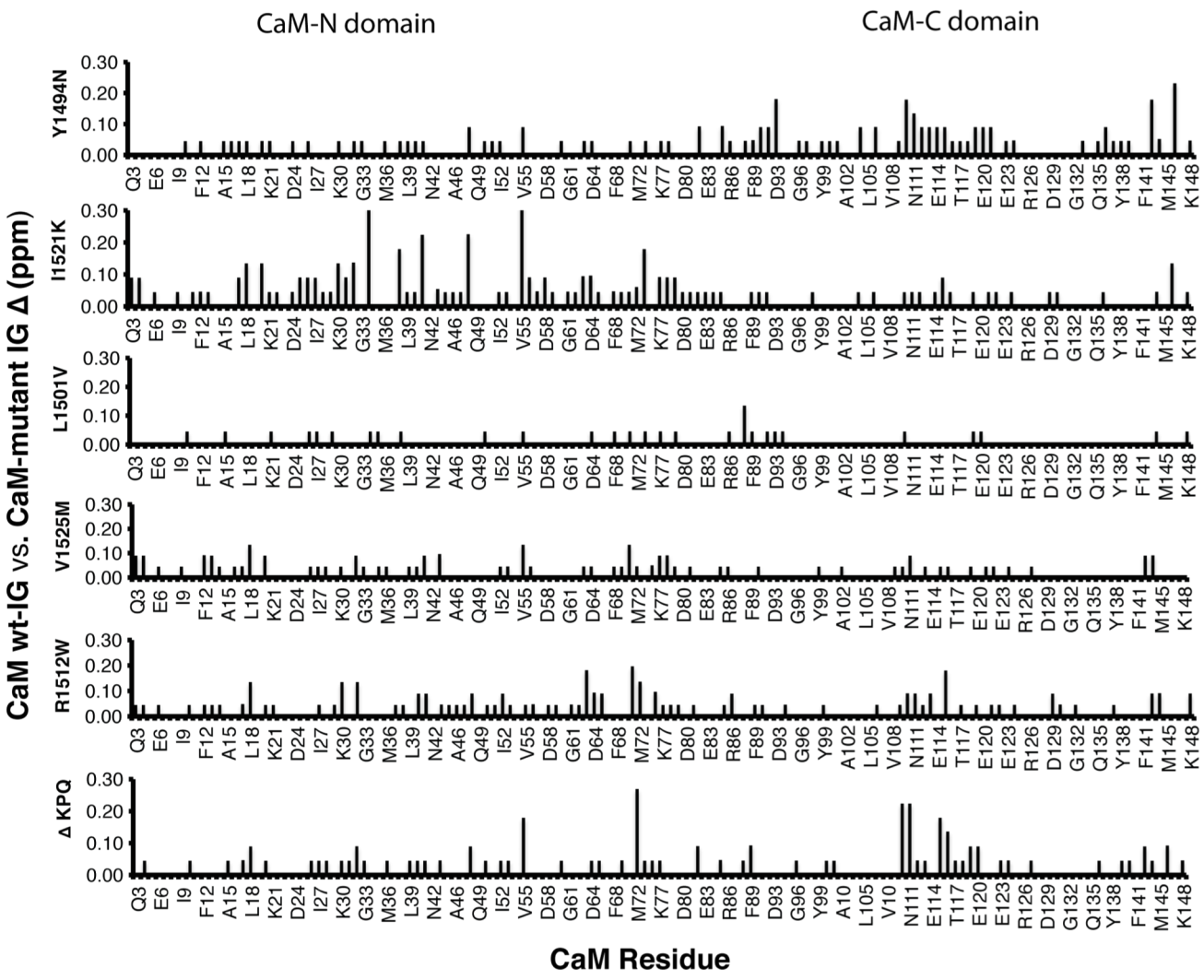

Fig. S10. Related to Fig. 5. **CaM binding to $Na_V1.5$-IG mutations**. Plots of changes in chemical shifts for Ca^{2+}-CaM binding to NaV1.5-IG peptides containing individual disease associated mutations. Values are shown as the difference compared to CaM binding wild type IG peptide.